ISSN 2091-5527
№ 2/2025

O‘zbekiston

Kompozitsion Materiallar

Ilmiy-texnikaviy va amaliy jurnali

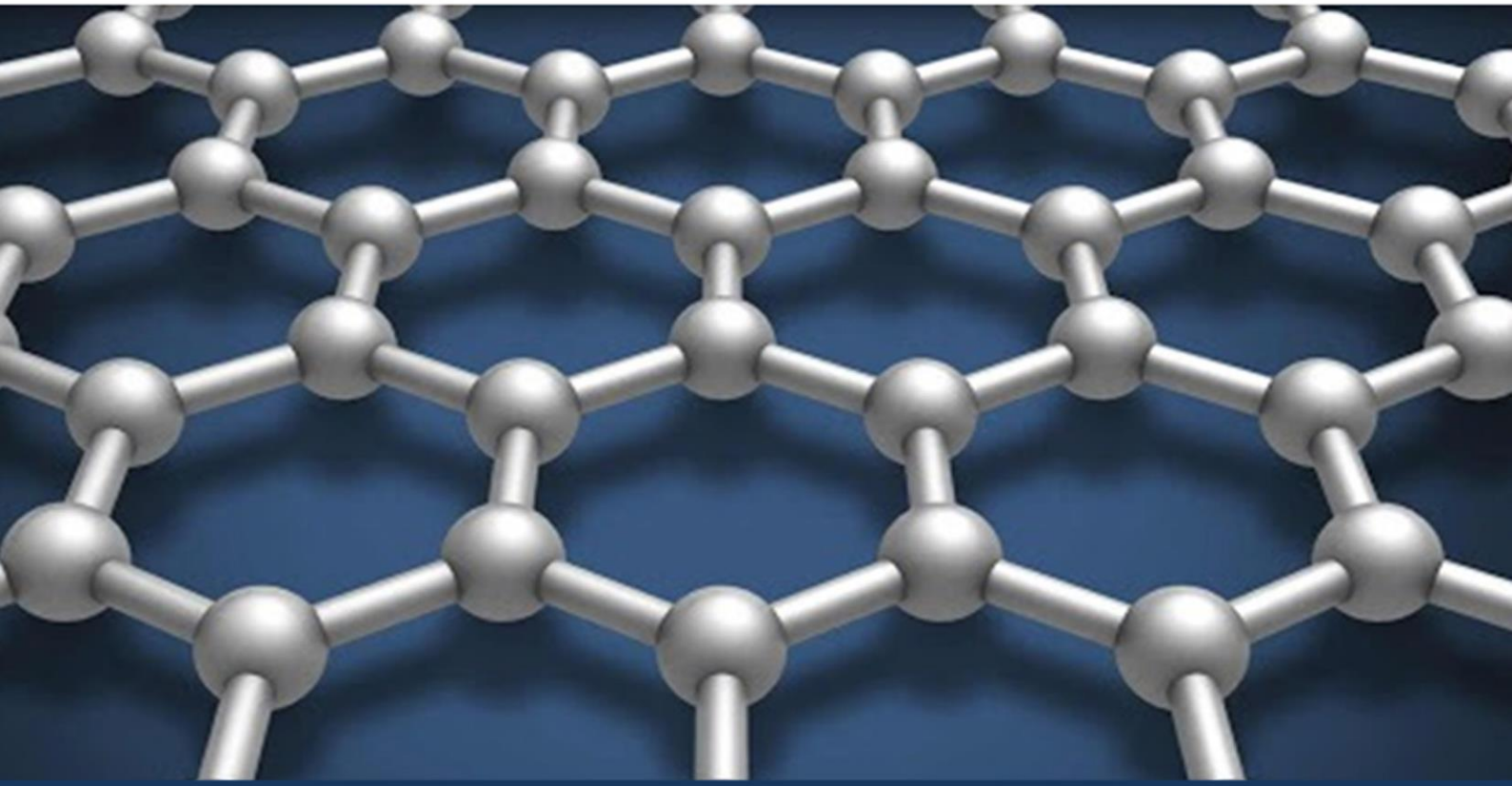

Узбекский научно-технический и производственный журнал

Композиционные материалы

18-CROWN-6 BASED SUPRAMOLECULAR STRUCTURE, Z-SCAN, HIRSHFELD SURFACE ANALYSIS NONLINEAR OPTICAL PROPERTIES

[1]Samandarov Elyorbek Shonazar ugli, [2]Ibragimov Aziz Bakhtiyarovich, [2]Yakubov Yuldosh Yusupboevich, [3]C.Balakrishnan, [2]Safarov Azamat Rasul o'g'li

[1]Khorezm Mamun branch of Uzbekistan Academy of Sciences, E-mail: samandarove6@gmail.com
[2]Institute of General and Inorganic Chemistry of Uzbekistan Academy of Sciences
[3]Department of Chemistry Erode Sengunthar Engineering College Erode, India

Abstract. Self-assembled supramolecular cocrystals of 18-crown-6. pyridine-3-ylmethanamine have been synthesized from 18-crown-6 (18C6) and pyridine-3-ylmethanamine (stoichiometric ratio 1:2). The single-crystal X-ray analysis revealed the crystal structure, indicating a monoclinic system with the centrosymmetric space group Pn. The assembly of the supramolecular structure primarily relies on N-H•••O and O-H•••O interactions. Characteristic functional groups were identified using FT-IR and micro-Raman spectral analyses. Additionally, the diffuse reflectance spectrum estimated a direct bandgap energy of 2.84 eV. The cocrystal exhibited fluorescent emission in the solid state at room temperature as observed in photoluminescence studies. Analysis utilizing Hirshfeld surface and fingerprint plots unveiled close contacts resulting from robust interactions in the crystal packing. The third-order nonlinear optical properties of the crystal grown were determined using a single-beam Z-scan technique.

Keywords.pyridin-3-ylmethanamine;1,4,7,10,13,16 hexaoxacyclooctadecane ; 1,4, 7,10,1 3,16-hexaoxacyclooctadecane, pyridin-3-ylmethanaminium salt; hydrogen bond; crystal data; FT-IR spectroscopy.

Introduction. Crown ethers are pivotal in supramolecular and coordination chemistry due to their ability to form host-guest complexes with unique structures and diverse bonding interactions[1-3]. Ammonium-crown ether-based organic-inorganic assemblies have been extensively studied [4-5], where the stability of these complexes depends on the crown ether size and the nature of the protonated ammonium cation (e.g., NH_4^+, RNH_3^+). A key structural feature is the encapsulation of the $–NH_3^+$ group within the crown ether cavity [6-7]. Supramolecular networks arise from weak intermolecular interactions, including hydrogen bonds, charge transfer, and van der Waals forces[8]. These materials find applications in data storage, capacitors, sensors, and optical devices [9-11]. Third-order nonlinear optical properties of the crystal ere examined by the Z-scan technique. Hirshfeld surface analysis was used to quantify intra- and intermolecular interactions[12].

Experimental. Single crystal X-ray structure analysis. The crystal structure was elucidated by single-crystal XRD analysis. Crystallographic data and details of the refinement parameters are listed in Table-1. Information of plane spacing for monoclinic structure crystal systems.

$$\frac{1}{d^2} = \frac{1}{sin^2\beta} \cdot \left(\frac{h^2}{a^2} + \frac{k^2\, sin^2\beta}{b^2} + \frac{l^2}{c^2} - \frac{2hl\cos\beta}{ac}\right)$$

The selected hydrogen bonds, bond distances and bond angles are listed in Tables 2-4. The ORTEP and packing diagram of 18C6•2(P3MA)•2(H_2O) are given in Fig-1. It crystallizes in the monoclinic system with centric space group Pn with Z = 2. The asymmetric unit consists of half 18C6, electron density peak is found near heavy atom iodine. Crystal is a layered type that cannot be separated. This caused bad data quality and high wR_2 value.Most of the amine/ammonium (R-NH_2, R-NH_3^+, etc.) containing crown ether complexes form N─H•••O/N-H•••O type of hydrogen bonds [15–17]. In the present study, the hydrogen bonds are only OW─H•••O18C6 because of the inclusion of water molecules in the crown ether cavity. There is no contact between the -NH_2 group and oxygen atoms in 18C6 because -NH_2 groups form the intramolecular hydrogen bonds.

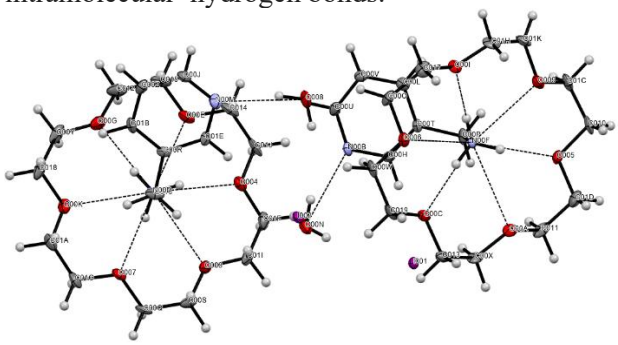

Fig-1. (a) ORTEP drawing of the intermolecular H-bonds and (b) Nonlinear optical (NLO) materials. 1,4,7,10,13,16-hexaoxacyclooctadecane, pyridin-3-ylmethanaminium salt. molecule. Thermal ellipsoids are drawn with the 50% probability level.

Table -1

Crystal data and structure refinement for $[(P3MA)_2^+ \cdot 2(18C6)] \cdot 2H_2O$.

Identification code	exp_393_CB08_auto
Empirical formula	$C_{36}H_{68}I_2N_4O_{14}$
Formula weight	1034.74
Temperature/K	107(5)
Crystal system	Monoclinic
Space group	Pn
a/Å	12.70250(10)
b/Å	9.45940(10)
c/Å	19.25390(10)
α/°	90
β/°	92.3510(10)
γ/°	90
Volume/Å^3	2311.56(3)
Z	2
ρ_{calc}g/cm^3	1.487
μ/mm^{-1}	11.216
F(000)	1060.0
Crystal size/mm^3	0.14 × 0.12 × 0.11
Radiation	Cu Kα (λ = 1.54184)
2Θ range for data collection/°	4.594 to 143.192
Index ranges	-15 ≤ h ≤ 15, -11 ≤ k ≤ 11, -23 ≤ l ≤ 23
Reflections collected	45306
Independent reflections	8957 [R_{int} = 0.0551, R_{sigma} = 0.0348]
Data/restraints/parameters	8957/2/520
Goodness-of-fit on F^2	1.040
Final R indexes [I>=2σ (I)]	R_1 = 0.0299, wR_2 = 0.0788
Final R indexes [all data]	R_1 = 0.0299, wR_2 = 0.0788
Largest diff. peak/hole / e Å^{-3}	1.36/-1.55
Flack parameter	0.000

Table-2

Hydrogen bonds for $[(P3MA)_2^+ \cdot 2(18C6)] \cdot 2H_2O$. ($A^0$); R = 0.03.

D-H•••A	d(D-H)	d(H•••A)	<DHA	d(D•••A)	Symmetry
O(008) – H(00Y) •••N(00M)	0.8700	2.0200	2.866(6)	164.00	
N(00D) – H(00S) ••• O(003)	0.9100	2.5100	2.994(5)	114.00	
N(00D) – H(00S)••• O(007)	0.9100	2.0000	2.817(5)	149.00	
N(00D) – H(00S)••• O(00K)	0.9100	2.6000	2.918(5)	101.00	
N(00D) – H(00T) •••O(004)	0.9100	1.9900	2.876(6)	165.00	
N(00D) –H(00T) •••O(00E)	0.9100	2.4100	2.934(5)	117.00	
N(00D) – H(00W)•••O(00G)	0.9100	1.9900	2.892(5)	174.00	
N(00D) – H(00W)••• O(00K)	0.9100	2.5000	2.918(5)	109.00	
N(00F) – H(00K) •••O(006)	0.9100	2.4900	2.959(5)	113.00	
N(00F) –H(00K)••• O(00C)	0.9100	1.9500	2.849(5)	169.00	
N(00F) – H(00L)••• O(009)	0.9100	2.5500	2.898(5)	103.00	
N(00F)–H(00L)•••O(00I)	0.9100	2.0000	2.906(5)	177.00	
N(00F)–H(00M) •••O(005)	0.9100	2.0100	2.828(5)	149.00	
N(00F)–H(00M) ••• O(009)	0.9100	2.4900	2.898(5)	107.00	
N(00F)–H(00M)•••O(00A)	0.9100	2.5800	3.012(5)	109.00	
O(00N)– H(G) •••N(00B)	0.87(8)	2.11(8)	2.914(6)	154(8)	**1/2+x,1-y,1/2+z**

Hirshfeld surface analysis. Description of the Hirshfeld surface analysis is quite detailed and informative. To summarize, Hirshfeld surface analysis is a powerful tool used in crystallography to visualize and analyze intermolecular interactions within a molecular structure. The coloring scheme (red, white, and blue) provides a clear representation of the electron density distribution and the nature of intermolecular contacts [13].

The creation of these surfaces involves partitioning the space enclosed by the crystal using the Hirshfeld ratio, where the procrystal is effectively delineated by employing a promolecule characterized by an electron density of 0.5[13-14]. The Hirshfeld surface is defined as the region in space where the ratio of the molecule's electron density (P_{mol}) to the total electron density $\rho_{total} = \rho_{mol} + \rho_{env}$ equals 0.5

$$\frac{\rho_{mol}(r)}{\rho_{mol}(r) + \rho_{env}(r)} = 0.5$$

Fingerprint plots are graphical representations of the intermolecular interactions in the crystal. Fingerprint plots provide a quantitative measure of the distribution of intermolecular contacts.Peaks in the fingerprint plot correspond to specific types of interactions.Hydrogen bonds-appear as sharp spikes at small de values (external distances).Van der Waals contacts-appear as broader peaks[15-16].

π-π stacking-often manifests as regions with intermediate di and de values.

They show the distribution of distances between pairs of points on the Hirshfeld surface and their nearest neighbors. The probability distribution of these distances is often expressed as:

$$P(d_i, d_e) = \frac{1}{N} \sum_{points\ on\ surface} \delta\,(d_i - d_i^{point})\delta(d_e - d_e^{point})$$

d_i and d_e-distances to the nearest nuclei inside and outside the molecule, respectively.

N-total number of points on the Hirshfeld surface; δ-dirac delta function.

The normalized contact distance, referred to as d_{norm}, is calculated by considering perspectives from both the exterior and interior of the surface, as outlined below:

$$d_{norm} = \frac{d_i - r_i^{vdW}}{r_i^{vdW}} + \frac{d_e - r_e^{vdW}}{r_e^{vdW}}$$

d_i -distance from a point on the Hirshfeld surface to the nearest nucleus inside the molecule.d_e-distance from a point on the Hirshfeld surface to the nearest nucleus outside the molecule (in the environment).

r_i^{vdW} - Van der Waals radius of the atom inside the molecule.

r_e^{vdW}-Van der Waals radius of the atom in the environment.

Quantitative analysis of the Hirshfeld surface revealed that the total volume was 599.64 Å^3 and the surface area was 470.26 Å^2. Generally, larger volume and surface area indicate more extensive intermolecular bonding and interactions within crystal structure. The crystal structure was analyzed using Hirshfeld surface analysis. The normalized contact distance d_{norm} ranged from -0.1281 to 1.4477 a.u.

Overall, the Hirshfeld surface analysis supplied useful perception into the intermolecular interactions and packing within the crystal structure of (NLO), highlighting the distribution of electron density and the nature of the non-covalent bonding interactions.

The 2D fingerprints of the Hirshfeld surface are shown in Fig-1. Analysis of these fingerprint plots revealed the presence of interactions between nine different homo- and heteroatomic contacts within and between the molecules that contribute to the overall crystal packing. The most prominent intermolecular interactions were H•••H contacts, which accounted for 57.8% of the Hirshfeld surface. This indicates a significant role of hydrogen bonding in stabilizing the crystal structura.

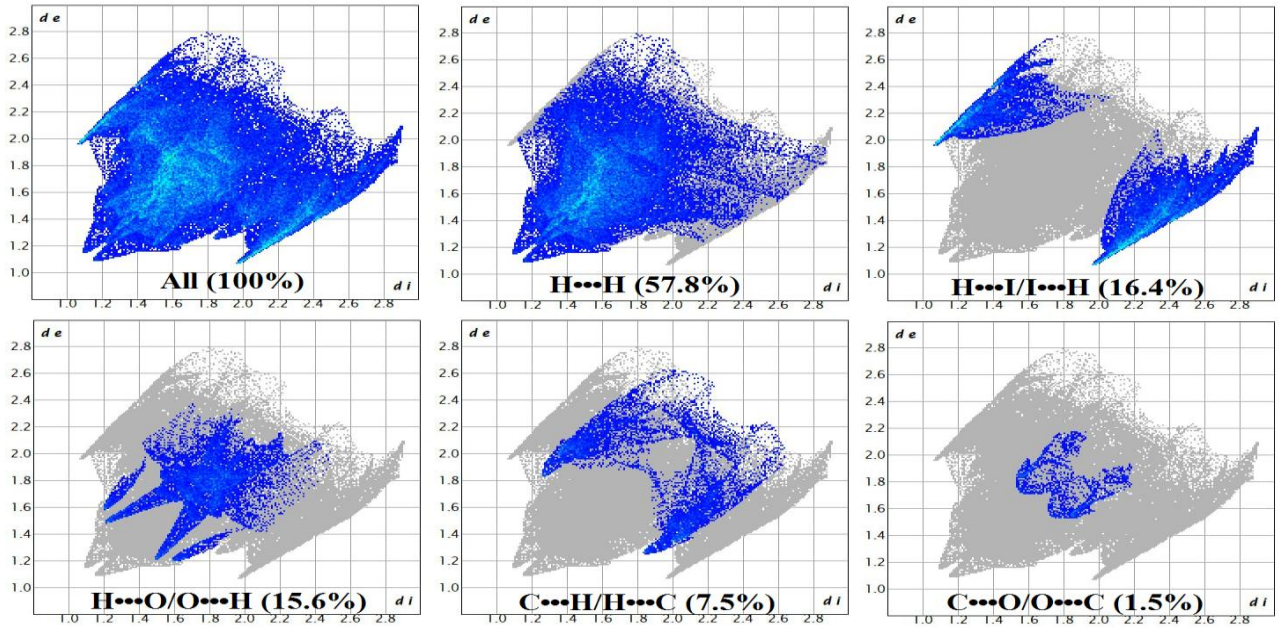

Fig-1. Hirschfeld surface fingerprint representation, contribution of interactions to surface formation

The second largest contributor was H•••I/I•••H contacts, making up 16.4% of the surface. These close hydrogen-hydrogen interactions also play an important role in the intermolecular packing. Other notable contributions include H•••O/O•••H contacts (15.6%), C•••H/H•••C contacts (7.5%), and C•••O/O•••C contacts (1.5%). These reflect the various van der Waals and dipole-dipole interactions present in the crystal.Hirshfeld surface, demonstrating the diversity of intermolecular interactions stabilizing the crystal structure of compound (NLO).

REFERENCES

1. Balakrishnan C. et al. Crystal structure and third-order nonlinear optical properties of supramolecular cocrystals of 18-crown-6 with 5-aminoisophthalic acid //Journal of Materials Science: Materials in Electronics. – 2024. – T. 35. – №. 8. – C. 614.
2. Chellakarungu B. et al. 18-Crown-6 based supramolecular structure, hydrogen bonding behaviour and its nonlinear optical properties. – 2023.
3. Guo M., Zhao M. M. 4-Bromoanilinium perchlorate 18-crown-6 clathrate //Structure Reports. – 2010. – T. 66. – №. 11. – C. o2836-o2836.
4. Vaganova T. A. et al. Polyhalogenated aminobenzonitriles vs. their co-crystals with 18-crown-6: amino group position as a tool to control crystal packing and solid-state fluorescence //CrystEngComm. – 2022. – T. 24. – №. 5. – C. 987-1001.
5. Wahan S. K., Bhargava G., Chawla P. A. Role of crown ethers as mediator in various chemical reactions //Ionic Liquids, Deep Eutectic Solvents, Crown Ethers, Fluorinated Solvents, Glycols and Glycerol. – 2023. – C. 145.
6. Merzlyakova E. et al. 18-Crown-6 coordinated metal halides with bright luminescence and nonlinear optical effects //Journal of the American Chemical Society. – 2021. – T. 143. – №. 2. – C. 798-804.
7. Shishkanova T. V. et al. Electrochemical sensor for phenylpropanolamine based on oligomer derived from 3-hydroxybenzoic acid with dibenzo-18-crown-6 //Journal of Electroanalytical Chemistry. – 2021. – T. 882. – C. 114963.
8. Bujor A. et al. Synthesis and Structural Analysis of a Nitrobenzofurazan Derivative of Dibenzo-18-Crown-6 Ether //Chemistry. – 2022. – T. 4. – №. 4. – C. 1696-1701.
9. Guezane-Lakoud S. et al. 2-Hydroxymethyl-18-crown-6 as an efficient organocatalyst for α-aminophosphonates synthesized under eco-friendly conditions, DFT, molecular docking and ADME/T studies //Journal of Biomolecular Structure and Dynamics. – 2024. – T. 42. – №. 7. – C. 3332-3348.
10. Tzeng B. C. et al. Luminescent Pt (II) complexes containing (1-aza-15-crown-5) dithiocarbamate and (1-aza-18-crown-6) dithiocarbamate: mechanochromic and solvent-induced luminescence //Inorganic Chemistry. – 2022. – T. 62. – №. 2. – C. 916-929.
11. Balakrishnan C., Vinitha G., Meenakshisundaram S. P. Novel C-H•••O hydrogen-bonded supramolecular complexes of 18-crown-6 with 1-alkylpyridinium iodide and its amino derivatives: Third-order nonlinear optical properties and Hirshfeld surface analysis //Journal of Molecular Structure. – 2022. – T. 1253. – C. 132310.
12. Adhami A. et al. Extraction of metal ions from water using a novel liquid membrane containing ZIF-8 nanoparticles, an ionic liquid, and benzo-18-crown-6 //Environmental Science: Water Research & Technology. – 2025.
13. Wineinger H. B. et al. Coordination Chemistry and Photoluminescence of Sm (II) Dibenzo-24-crown-8 Complexes //Inorganic Chemistry. – 2025.
14. Liu Y. et al. Esterified phenylalanine supramolecular motion: Anion order–disorder rotation induced reversible phase transition and dielectric-ferroelectric properties //Journal of Molecular Structure. – 2025. – T. 1328. – C. 141283.
15. Dhanalakshmi M. et al. Synthesis, structure, third-order nonlinear optical properties and Hirshfeld surface analysis of 18-crown-6 with dimethylpyridin-1-ium iodide isomers //Solid State Sciences. – 2024. – T. 157. – C. 107704.
16. Balakrishnan C. et al. Supramolecular structure of bis (1-methyl-1, 3, 5, 7-tetraazatricyclo [3.3. 1.13, 7] decan-1-ium) 2, 5-dicarboxybenzene-1, 4-dicarboxylate: Synthesis, spectral, structural and third-order nonlinear optical properties //Journal of Molecular Structure. – 2024. – T. 1296. – C. 136822.

4. Прикладные, экономические и экологические аспект применения композиционных материалов

5. Методы исследовании, приборов и оборудований композиционных материалов